Available online at www.sciencedirect.com

jmr&t Journal of Materials Research and Technology

www.jmrt.com.br

Original Article

The role of ausforming in the stability of retained austenite in a medium-C carbide-free bainitic steel

M. Zorgani[a,*], Carlos Garcia-Mateo[b], M. Jahazi[a,*]

[a] Department of Mechanical Engineering, École de Technologie Supérieure, 1100 Notre-Dame Street West, Montreal, QC, H3C 1K3, Canada

[b] National Center for Metallurgical Research (CENIM-CSIC), Avda. Gregorio del Amo 8, Madrid 28040, Spain

ARTICLE INFO

Article history:
Received 23 March 2020
Accepted 18 May 2020

Keywords:
Ausforming
Retained austenite stability
Carbide-free bainite
Martensite
Dilatometer signal

ABSTRACT

In this work, the influence of thermomechanical treatments, consisting of a combination of ausforming followed by isothermal holding and cooling to room temperature, on the stability of retained austenite of a carbide-free medium carbon-high silicon steel was investigated. The amount of retained austenite and its transformation to martensite for a range of ausforming treatments was determined by means of X-ray diffraction, dilatometry signal analysis, and metallographic investigation. Different amounts of deformations were applied at 600 °C in the austenite region prior to fast cooling into the bainitic transformation region. Four isothermal temperatures (325, 350, 375, and 400 °C) with a holding time of 1800 s were selected to estimate the extent of the stability of the retained austenite after the completion of the bainitic transformation. The results show that the deformation-free austenite was more stable for the samples isothermally treated at temperatures between 325 and 350 °C. However, the decomposition of retained austenite to martensite during cooling to room temperature increased for isothermal holding temperatures above 350 °C. It was found that the stability of retained austenite was a function of the temperature and percent deformation, and the critical temperature and percent deformations were determined. It was also found that ausforming enhanced the formation of blocky-shaped retained austenite for isothermal holdings above 350 °C, resulting in a decrease in retained austenite stability. The results were analyzed in terms of the influence of thermomechanical conditions on bainitic transformation and its impact on the transformation of retained austenite to martensite.

1. Introduction

Nanostructured carbide-free bainite (CFB) in high-carbon (~1.0 wt.%) silicon-rich steel has a superior combination of strength, toughness, and ductility due to its composite-like microstructure [1,2]. The excellent combination of these properties comes from the unique microstructure which consists of thin bainitic ferrite plates, which give the strength, and the stable metastable retained austenite that enhances the toughness and ductility through the transformation induced plasticity phenomenon (TRIP effect) [3,4]. Therefore, it is essential that the CFB steel microstructure contains only bainitic ferrite and retained austenite without the presence of martensite before being introduced into industrial applications. However, the steel's poor weldability, caused by its high carbon content, limits its use in many industrial sec-

* Corresponding authors.
https://doi.org/10.1016/j.jmrt.2020.05.062

tors. On the other hand, it is difficult to obtain a very fine bainitic microstructure in low or medium carbon steels since the martensite start temperature is relatively high. One of the alternative ways of obtaining such fine morphology is to work-harden the unstable austenite before the bainitic transformation, using ausforming process [5,6].

There are two types of retained austenite morphologies in CFB. The first one is film-like and located between the bainite plates. These films become stable due to carbon enrichment from the bainitic plates. The other one is the low-carbon blocky-shaped retained austenite located between the bainite sheaves. The stability of the retained austenite could be quantified by estimating the amount of transformed martensite from the decomposition of the remaining austenite at the end of the bainitic transformation [7]. The formation of untempered martensite is of critical importance as it could act as crack initiation sites [8–10]. It has been reported that the stability of the retained austenite is affected by its carbon content, morphology, and size [11–13]. On the other hand, the bainitic transformation temperature and the deformed state of supercooled austenite can also alter the above factors and therefore influence the retained austenite stability [14,15].

In pure isothermal bainitic transformation (deformation-free austenite), the probability of the decomposition of retained austenite to martensite is more significant when the bainitic transformation takes place at higher temperatures [16]. Specifically, it has been reported that the stability of blocky-shape retained austenite was higher when the isothermal temperatures were below 400 °C, but that transformation to fresh martensite occurred above 400 °C [9]. Several authors [17–19] have reported that the amount of retained austenite that could be stabilized, at the end of isothermal holding, depends on the degree of carbon enrichment during the bainitic reaction. Therefore, the higher the carbon enrichment, the more stable it would be the retained austenite [20,21]. Another research in low C–Mn steel [22] reported that an increase in the bainitic isothermal temperature, from 330 to 390 °C, enhanced the stability of retained austenite and increased its amount at the end of the bainitic transformation. The authors associated the higher stability of retained austenite at higher bainitic transformation temperatures to higher diffusion of C and Mn. Hence, the bainitic isothermal temperature appears to have a substantial effect on the stability of blocky shape retained austenite and therefore needs further investigation.

It has been reported that the deformation of austenite prior to the bainitic transformation, results in a reduction in the retained austenite block size and an increase in its volume fraction after the isothermal transformation [23,24]. Hu et al. [25] studied the effects of strain and ausforming temperature on the stability of retained austenite and found a direct relationship between the stability of the retained austenite and the applied plastic strain when the deformation temperature was above 300 °C. However, they reported that when the plastic strain reached 0.3, and the ausforming temperature was 300 °C, the correlation was inversed. Seo et al. [26], reported that ausforming of medium carbon steel at 600 °C, decreased the martensite start temperature, M_S, and stabilized the austenite during cooling to ambient temperatures and associated it with the effect of carbon diffusion on the stability of retained austenite.

Besides the effect of carbon diffusion, the stability of retained austenite has been analyzed in terms of mechanical stabilization through the introduction of a large number of dislocations into the microstructure when ausforming temperature is reduced [25,27,28]. Therefore, increasing the number of defects, such as dislocations, is expected to retard martensitic and/or bainitic transformations [27]. Bhadeshia et al. [28] reported that plastic deformation of austenite prior to its transformation, ausforming, hinders the growth of martensite or bainite and causes a reduction in the fraction of transformation in spite of an increased number density of nucleation sites.

However, in most of the above studies, little information is provided on the quantitative relationship between the stability of retained austenite due to the thermal and/or mechanical stabilization. Furthermore, whether the bainite transformation took place with or without the ausforming step, the stability of the retained austenite (i.e., its decomposition to martensite) has not quantified. Such information will be of great value for a better understanding of the contribution of ausforming to the stability of retained austenite in the final microstructure of CFB steels. The selection of suitable conditions for ausforming and bainitic transformation is crucial for obtaining the optimal amount and stability of the retained austenite that minimizes the amount of untempered martensite in the final stage of the bainitic transformation. The present research has been defined in this context and aims to systematically quantify the thermal and mechanical stability of retained austenite, obtained through ausforming followed by isothermal treatments of a carbide-free medium-C high-Si steel, during cooling to room temperature.

2. Experimental procedure and material

A rod of 300 mm diameter of a commercial-grade medium carbon steel Ovako 477L, with the nominal chemical composition of Fe–0.4C–1.7Si–1.5Mn–1.5Cr–0.4Mo (wt.%), was selected for this study. In order to reduce some of the experimental tests, the theoretical CCT diagram was calculated using JMatPro® simulation software [29]. Dilatometry tests were carried out using the DIL 805A/D-TA high-resolution dilatometer. The linear dilatation during the tests was recorded using a Linear Variable Differential Transducer (LVDT) attached to fused silica pushrods with a resolution of $\Delta L/°C = 0.05\ \mu m/0.05\ °C$ [30]. The temperature was monitored using type S thermocouples welded at the center of the sample. For pure isothermal treatments (non-ausformed), the quenching module of the dilatometer was used with cylindrical samples 10 mm in length and 4 mm in diameter. The thermomechanical treatments (TMT) were performed using the deformation module of the dilatometer for which cylindrical samples 5 mm in diameter and 10 mm in length were used. For deformation tests, molybdenum discs with a thickness of 1 mm were welded on both sides of the specimens to reduce the friction between the sample's cross-sectional surface and the deformation anvils (SiN). All the samples were prepared using wire-based Electro Discharge Machining (EDM) along the

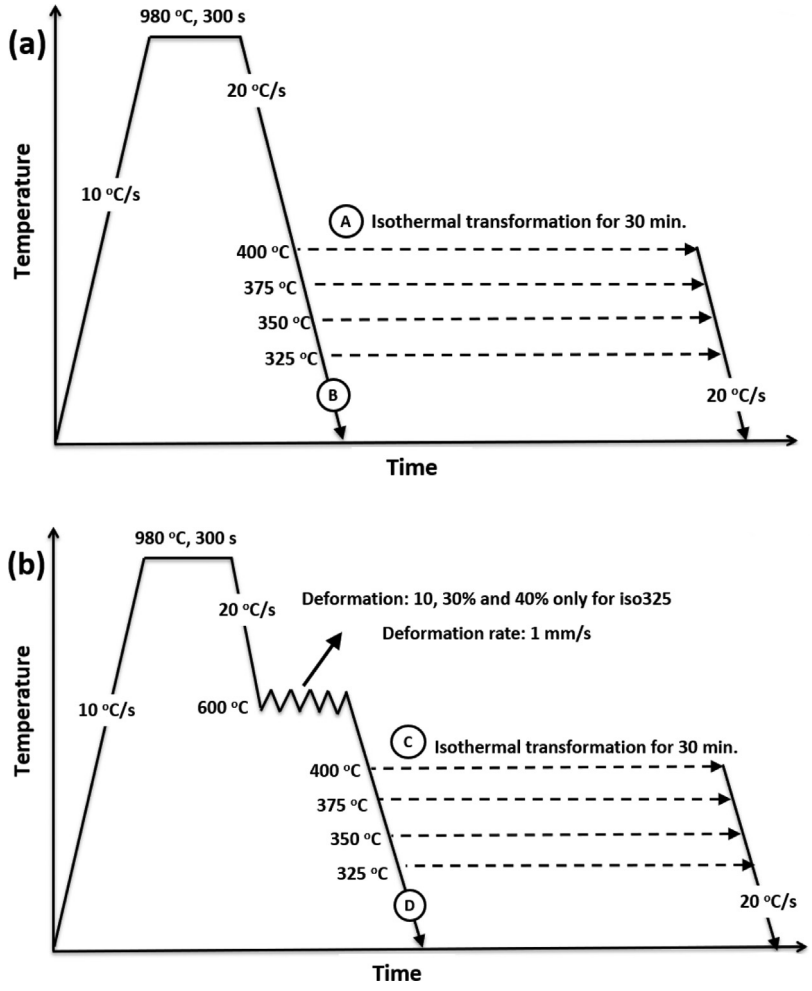

Fig. 1 – Scheme of the performed tests and their corresponding conditions: (a) non-ausformed condition, (b) ausformed condition with different percent deformation.

rolling direction of the as-received bar. Four different treatment routes (A, B, C, and D) were applied, as shown in Fig. 1a and b. In route (A) (non-ausformed, Fig. 1a), the samples were cooled with a cooling rate of 20 °C/s from the austenitization temperature to the isothermal treatment temperature, ranging from 400 to 325 °C. They were then further cooled to room temperature at a cooling rate of 20 °C/s. Samples produced through route (A) are considered as a reference for comparison purposes with ausformed samples. In route (C) (ausformed, Fig. 1b), the samples were first deformed at 600 °C, before applying the isothermal heat treatment under the same conditions as those in route (A). Routes (B) and (D) were used to measure the M_S of the non-ausformed, route (B), and ausformed samples with different percent deformations, route (D).

Microstructural examinations were conducted in the longitudinal-central section of the samples using standard metallography techniques. Sample preparation included grinding and polishing up to 1 μm diamond paste, followed by a cycle of etching (3% Nital for 10 s) and polishing to remove the deformed layer that formed during the grinding process [31]. Confocal laser microscopy (Olympus-LEXT4100) and field emission scanning electron microscopy (Hitachi SU-8230, FE-SEM) were used for microstructural characterizations. The volume fraction of retained austenite ($V_{\gamma R}$) and its carbon content ($C_{\gamma R}$) after isothermal transformation were determined by X-ray diffraction (XRD) using a X'PERT PANalytical diffractometer with Co Kα radiation. The operational conditions consisted of an acceleration voltage of 45 kV, a 2θ scan range from 30° to 120°, and a step size of 0.05°.

Retained austenite volume fraction determination, $V_{\gamma R}$, was made based on a direct comparison method [32] and consisted in first determining its lattice parameter (α_γ), in (Å), from the diffractograms according to Eq. (1). Then, using the average integrated intensities of ferrite (I_α) and austenite (I_γ) peaks, $V_{\gamma R}$, and $C_{\gamma R}$, were calculated in (wt.%) as per Eqs. (2) and (3), respectively.

$$\alpha_\gamma = \frac{\lambda\sqrt{h^2+k^2+l^2}}{2\sin\theta} \quad (1)$$

$$V_{\gamma R} = \frac{1.4I_\gamma}{I_\alpha + 1.4I_\gamma} \quad (2)$$

$$C_{\gamma R} = \frac{\alpha_\gamma - 3.547}{0.046} \quad (3)$$

In the above equations, λ, (hkl), and θ is the wavelength of the radiation, the three Miller indices of a plane, and the Bragg angle, respectively.

As already mentioned, the stability of retained austenite is defined as its ability to resist decomposition to bainite during isothermal transformation or to martensite during cooling to room temperature. However, in this study, only the later phenomenon will be investigated. Therefore, it is of critical importance to accurately determine the amount of martensite formed ($V_{\alpha m}$) from the austenite during cooling to room temperature after the isothermal holding. To this end, two different methods were used: The first method was based on the change in the slope of dilatometry signals, as described in [33]. In this method, the net relative change in length (RCL) at room temperature is compared with the net RCL of martensitic transformation, which is considered as a reference for non-ausformed (Q-00) and ausformed (Q-10, Q-30, and Q-40) samples. The reference dilatation is then correlated to the amount of transformed martensite determined by XRD (i.e., $V_{\alpha m} = 100 - V_{\gamma R(\mathrm{XRD})}$). For example, the net dilatation, $\Delta(\Delta L/L_o)$, corresponding to 92% martensite for the non-ausformed condition (Q-00), is about 0.97%. The amount of martensite, formed during cooling after the isothermal treatment, is calculated by comparing the recorded net RCL with that of the reference net RCL. The results thus obtained, will be designated as $V_{\alpha m(\mathrm{dil})}$, where the subscript (dil) refers to dilatometry-based results. It must be noted that all dilatometry tests were repeated three times, and the presented RCL values are the average of the three tests.

The second method is based on microstructural identification of blocky-shape retained austenite from the martensite within the martensite/austenite (M/A) islands, as described in Refs. [10,21,34,35]. For each test condition, at least four SEM micrographs at a 4000 magnification were used, and for accuracy, the area fraction measurement was repeated five times for each image. The volume fraction of transformed martensite, $V_{\alpha m(\mathrm{SEM})}$, was then determined by calculating the area fraction occupied with martensite in the micrographs using the image analysis software, MIP4 [36]. The method consisted of, first, determine the fraction of M/A constituent in SEM images. Then, the darkest/featured region within them (martensitic phase) was subtracted, and finally, the volume percentage of the martensite was determined.

The Vickers microhardness was measured using a 1 kg load 1 kgf, and a dwell time of 15 s. The hardness values reported were taken at various locations around the center of the sample and sufficiently apart from each other to avoid interaction effects. The mean value and standard deviation of hardness measurements were obtained by statistical analysis using five hardness readings.

For simplification, the sample designation is as follows: the first three digits of the sample designation code (xxx-xx) represent isothermal temperature, while the second two digits after the dash represent the amount of deformation at 600 °C. For example, 325-30 corresponds to the sample with 30% plastic deformation, followed by isothermal treatment at 325 °C, whereas, 325-00 indicates isothermal treatment at 325 °C with no deformation. For quenching samples, Q-00 represents the quenching treatment without deformation, and Q-10, Q-30, and Q-40 are quenching treatments after the sample was deformed with 10, 30, and 40% plastic deformation at 600 °C.

3. Results and discussions

3.1. *Selection of thermomechanical treatment conditions*

The critical transformation temperatures Ac_1 and Ac_3 were found experimentally, as illustrated in Fig. 2a, using heat treatment parameters shown in Fig. 1a (route (B)), to be 840 and 930 °C, respectively. As shown in the same Fig. 2a, a cooling rate of 20 °C/s is sufficient to activate martensitic transformation avoiding any other previous transformation. The martensite start temperature, M_S, was determined to be 310 ± 5 °C using the tangent method [37].

Based on the above results, isothermal transformation treatments at 325, 350, 375, and 400 °C were selected to study the bainitic transformation during isothermal holding. Furthermore, an isothermal time of 1800 s was selected in all conditions to ensure the end of the bainitic transformation in agreement with experiments previously reported in the literature [31,38,39].

The first set of calculations using JMatPro® software [29] showed that the bay between the ferrite/pearlite and the bainite regions is located in the temperature interval of 500–600 °C and also that the critical cooling rate is 1 °C/s (Fig. 2b). Such temperature would be ideal to plastically deform austenite prior to bainitic transformation, as no other transformation would be expected to interfere. In order to ensure the validity of the calculations, selected isothermal dilatometry tests at 500, 600, and 700 °C, using the same conditions as those previously described, have been performed. As expected from the calculations and the dilatometric curve is shown in Fig. 2c, reveal the absence of any relative change in length, thereby confirming that no phase transformation occurred at 500 and 600 °C after 1800 s dwell time. Furthermore, the microstructure examination of the samples reported in Fig. 2d showed that only martensite was present at room temperature. In contrast, at 700 °C, a ferrite–pearlite transformation started after about 700 s, which was also confirmed by metallographic analysis reported in Fig. 2d, where a mixture of pearlitic and martensitic phases was identified. Therefore 600 °C was selected as the ausforming temperature, where deformations between 10 and 30%, at a deformation rate of 1 mm/s, were applied. As will be described later, some experiments were conducted with a 40% deformation to validate the interpretations and the proposed mechanisms for the interpretation of the results. A summary of all test conditions is presented in Fig. 1a and b.

3.2. *Stability of retained austenite of non-ausformed samples (reference condition)*

3.2.1. *Dilatometry analysis*

Fig. 3 illustrates the dilatometry signals (RCL) for isothermally treated samples at 325, 350, 375, and 400 °C, and the quenched condition. Note that in the case of the isothermal treatments,

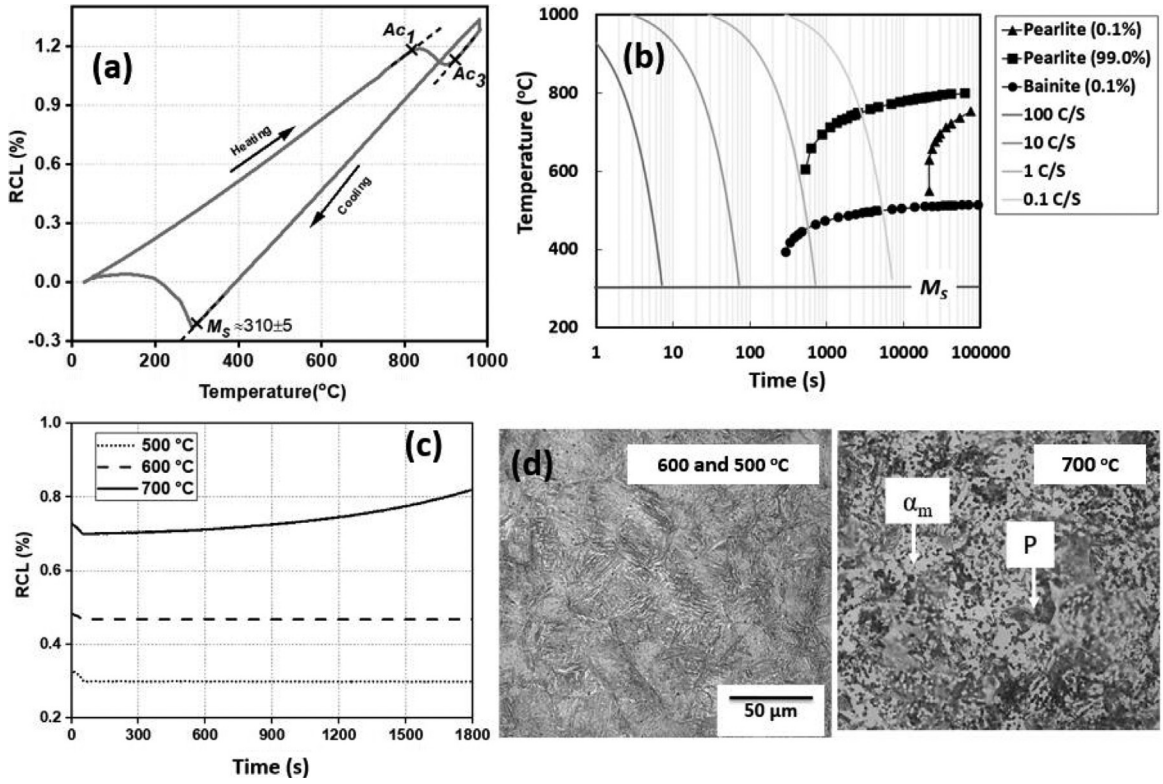

Fig. 2 – (a) The dilatation vs. temperature during the entire thermal simulation, (b) CCT diagram for 477L steel constructed by JMat-pro program, (c) dilatation–time curves for 500, 600 and 700 °C isothermal treatments, (d) optical micrographs for 500, 600, and 700 °C sample.

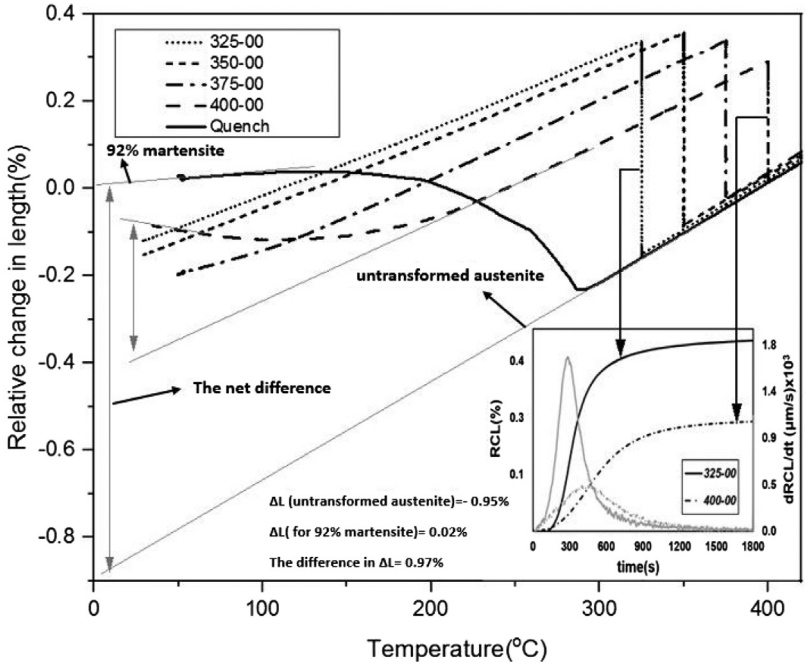

Fig. 3 – Relative change in length vs. temperature during the quenching to room temperature for different non-ausformed treatments, and image in bottom right is a relative change in length and transformation rate vs. time for the lowest (325 °C) and the highest (400 °C) isothermal temperatures.

any change in length is directly related to the formation of bainitic ferrite. As already mentioned, the selected isothermal holding time, 1800 s, was sufficiently long to allow for the bainite transformation to finish, as shown in the inserted curve in Fig. 3 corresponding to the isothermal transformation at 325 °C and 400 °C, i.e., the slowest and fastest of transformations. It is clear that the increment of dilatation values is negligible after about 1500 and that the curve has reached its steady-state (plateau) at that time, no more transformation. In the same inset of Fig. 3, the dilatation rate (first derivative curve), related to the transformation rate, is almost zero at 1500 s, further confirming that no more bainitic transformation could be observed after 1500 s. It must be noted that the increase in the RCL with the decrease in isothermal transformation temperature is in agreement with other results that the amount of bainitic ferrite, $V_{\alpha b}$, is higher when the transformation temperature is lower [28,40].

The obtained results on isothermal transformation at 325 and 350 °C (325-00 and 350-00), as shown in Fig. 3, also confirm that no martensitic transformation is occurring on cooling to room temperature, meaning that austenite present in the microstructure is sufficiently enriched in C to be stable, M_S less than room temperature. However, as the C enrichment in austenite decreases, by increasing the isothermal bainitic transformation temperature at 375 and 400 °C, it is clear that austenite transforms to martensite [28]. The first deviation in the dilatometric signal during cooling to room temperature represents the M_S of C-enriched retained austenite due to bainite transformation, as shown in Fig. 3. The results in Table 1 showed that the M_S decreased by about 50% (150 °C) and 27% (225 °C) for 375-00 and 400-00 samples, respectively, compared with the quenched condition (310 °C). As already explained, the deviation of the dilatation curve can be considered as an indicator of the extent of decomposition of retained austenite to martensite [41–43]. Note that the change in slope occurs more gradually as compared to that of the quenched sample, Fig. 3, and this is due to the more heterogeneous C distribution in the remaining austenite after bainitic transformation, with block-shaped and thin films of retained austenite having very different C contents [9,22,44]. In the as quench condition, a fraction of 92% of martensite was measured, see Table 1, which corresponds to a net difference in RCL of about 0.97 ± 1%, using the method described in the previous section, the fraction of martensite, $V_{\alpha m(\mathrm{dil})}$, was calculated for all conditions, and the results are reported in Table 1. Specifically, the amount of austenite transformed to martensite was almost twice when the temperature increased from 375 to 400 °C.

3.2.2. *XRD analysis*

The XRD diffractograms for the non-ausformed samples are reported in Fig. 4a where the presence of ferrite phases (α_b and α_m) (α-1 1 0), (α-2 0 0), (α-2 1 1), and austenite (γ-1 1 1), (γ-2 0 0), (γ-2 2 0) planes with no cementite peaks after bainitic transformation are revealed. These findings further confirm the dilatometric results on the phase transformation process at different isothermal holding temperatures. The corresponding fractions of the different phases and austenite carbon content ($C_{\gamma R}$) were also calculated and are given in Table 1 for comparison purposes. The results indicate that, as expected, the fraction of bainitic ferrite decreases (i.e., smaller RCL

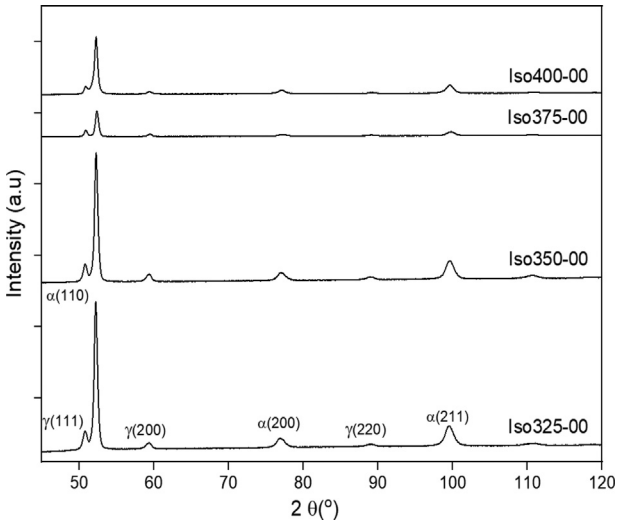

Fig. 4 – XRD diffraction spectrum of non-ausformed samples.

in Fig. 3) as transformation temperature increases; however, it appears that increasing the isothermal transformation by 25 °C (from 325 to 350 °C), had a limited effect on the variation of the bainite volume fractions. For instance, the variation in $V\alpha_b$ was less than 2.5%, leading to about 10% variation in $V\gamma_R$ as reported in Table 1. The obtained results suggest that martensitic transformation after isothermal transformation at 350 °C, and probably 325 °C, could not be detected by the dilatometry technique. As for the 375 and 400 °C transformation temperatures, there is an apparent decrease in the amount of transformed bainite, once the calculated amount of martensite, $V_{\alpha m(\mathrm{dil})}$, is considered. For example, the variation in $V\alpha_b$ was about 45% between 325-00 and 400-00 samples, while the variation in $V\gamma_R$ was about 25% for the same conditions due to its decomposition during cooling to room temperature as seen in Fig. 3.

During the bainitic transformation, austenite receives C from the surrounding C saturated bainitic ferrite, and it is expected that the level of C enrichment, $C_{\gamma R}$, increases with the amount of bainitic ferrite [45,46]. Although the results reported in Table 1 seems to go in that direction, it must be considered that such results were obtained at room temperature, where part of that austenite has transformed to martensite. Therefore, the actual level of C enrichment must be lower than the one obtained from XRD results reported in Table 1. In other words, the higher the amount of martensite, the lower would be the actual value of $C_{\gamma R}$ as compared to the one given in Table 1. For instance, using the lever rule, it was found that for the 400 °C testing condition, $C_{\gamma R}$ could be as low as 0.4–0.5 wt.% for martensite containing 0.2–0.3 wt.% of C.

3.2.3. *Microstructural and microhardness analysis*

SEM images of the non-ausformed samples at different temperatures are shown in Fig. 5a–d. At the lowest temperatures, 325 and 350 °C, the microstructure consists of plate-like bainite, retained austenite (in the form of films (γ_f) and blocks (γ_b)), and some dispersed martensite in the form of M/A constituents (Fig. 5a and b). As the transformation tem-

Table 1 – Volume fraction of different phases for non-ausformed and ausformed samples in (%): $V_{\alpha m(dil)}$ for martensite based on dilatometry, $V\alpha_{m(XRD)}$ (=100 − $V_{\gamma R}$), from XRD, $V_{\gamma R}$ retained austenite calculated by XRD, $V\alpha_b$ (=100 − $V_{\gamma R}$ − $V_{\alpha m(dil)}$) bainitic ferrite; the carbon content of retained austenite, $C_{\gamma R}$, in (wt.%) from XRD for, and the M_S in (°C).

TMT condition	Sample code	$V\alpha_{m(dil)}$	$V\alpha_{m(XRD)}$	$V_{\gamma R}$	$V\alpha_b$	$C_{\gamma R}$	M_S
Non-ausformed + quenching	Q-00	–	92 ± 2	8 ± 2	–	–	310 ± 5
Non-ausforming + austempering	325-00	0	–	14 ± 2	86 ± 2	1.22 ± 0.21	< RT
	350-00	0	–	16 ± 3	84 ± 3	1.23 ± 0.22	< RT
	375-00	16 ± 4	–	14 ± 3	70 ± 3	0.98 ± 0.11	150 ± 3
	400-00	29 ± 4	–	18 ± 2	53 ± 2	0.85 ± 0.13	225 ± 4
Ausforming + quenching	Q-10	–	89 ± 3	11 ± 3	–	–	310 ± 2
	Q-30	–	90 ± 2	10 ± 2	–	–	310 ± 2
	Q-40	–	86 ± 2	14 ± 2	–	–	300 ± 2
Ausforming + austempering	325-10	0	–	19 ± 2	81 ± 2	1.18 ± 0.20	< RT
	325-30	0	–	23 ± 5	77 ± 5	1.16 ± 0.25	< RT
	325-40	0	–	27 ± 2	73 ± 2	1.17 ± 0.15	< RT
	350-10	8 ± 3	–	19 ± 3	73 ± 3	1.05 ± 0.30	180 ± 2
	350-30	11 ± 5	–	18 ± 5	71 ± 5	0.95 ± 0.20	275 ± 3
	375-10	17 ± 6	–	17 ± 6	66 ± 6	0.93 ± 0.11	250 ± 2
	375-30	20 ± 4	–	16 ± 4	64 ± 4	0.90 ± 0.10	260 ± 3
	400-10	34 ± 4	–	19 ± 4	47 ± 4	0.88 ± 0.20	290 ± 2
	400-30	37 ± 4	–	18 ± 4	45 ± 4	0.82 ± 0.16	300 ± 4

perature increases, the bainitic ferrite morphology evolves from plate-like toward granular, and blocky shape austenite increase in number and size in detriment of the thin films, which are almost inexistent at 400 °C as seen in Fig. 5d.

Microstructural observations revealed that the decomposition of retained austenite to martensite always occurred within the blocky-shape retained austenite, including M/A islands, rather than the film-like ones, which has also been reported by Zhao et al. [41]. Thus, it is vital to understand the relationship between the size changes of the M/A constituents as a function of isothermal temperature and deformation. Table 2 summarizes the average size of the M/A constituents as well as the volume fraction of the martensitic phase obtained based on an electron microscopy examination of the samples for all testing conditions. The microhardness measurements are also reported for all conditions for comparison and validation purposes of the microstructural evaluations. It must be noted that the amount of $V\alpha_{m(SEM)}$ reported in Table 2, was estimated based on the observed variations in the contrasts between martensite and blocky-shaped austenite in the M/A constituent, as shown in Fig. 5e and in agreement with similar studies reported in the literature [10,21,34,47].

Metallographic examination revealed a small fraction (<5%) of *transformed martensite*, $\alpha_{m(SEM)}$ for lower isothermal temperatures of 325 and 350 °C. However, it must be noted that such a presence was not detected in the dilatometry tests shown in Fig. 3, probably due to its small percentage. In contrast, the dilatometric observations and XRD results of the tests at 375 and 400 °C revealed that the fraction of transformed martensite increased to about 15 and then 25%, respectively, with the increase in the test temperature from 375 to 400 °C. These findings further reinforce the argument that retained austenite after the bainitic transformation is not sufficiently stable at these temperatures. It is also worth noticing the good agreement between the volume fraction of martensite calculated by dilatometry, $V\alpha_{m(dil)}$, in Table 1, and the one by microstructure examination, $V\alpha_{m(SEM)}$, in Table 2.

The evolution of microhardness, shown in Table 2, reveals that for the undeformed samples, it decreases from 325 to 350 °C but starts to increase again when the test temperature increases to 375 and 400 °C. As reported in Table 2 and Fig. 5a, a small increase in bainitic ferrite fraction and finer microstructural features are observed in the 325-00 sample compared to the 350-00. It has been reported that the final strength of the microstructure in CFB steels is susceptible to the bainitic ferrite plate thickness [48]; therefore, the observed hardness drop between 325 and 350 °C could be related to such microstructural changes. In contrast, the presence of increasing amounts of martensite (as reported in Table 2 and Fig. 5c and d) is probably at the root cause for the observed hardness increase at higher isothermal holding temperatures.

3.3. *Stability of retained austenite of ausformed samples*

3.3.1. *Deformation behavior of supercooled austenite*

Fig. 6 shows the flow curves of the supercooled austenite obtained during compressive deformation at 600 °C (10, 30, and 40%) prior to bainitic transformation. As can be seen, a continuous work hardening is observed for al deformation levels. The absence of any softening in the stress–strain curve indicates that very little or no dynamic recrystallization has taken place under any of the tested experimental conditions. Therefore, only an increase in the dislocations density as a result of the applied plastic deformation has modified the microstructure.

Utilizing the Bergström model [49], it is possible to estimate the variation in dislocation density (ρ) of for medium carbon steels [50] as a function of the applied true strain (ε) as: [51]

$$\rho = \frac{U[1 - \exp(-\Omega\varepsilon)]}{\Omega} \tag{4}$$

$$\Omega = k\{Z\}^m \tag{5}$$

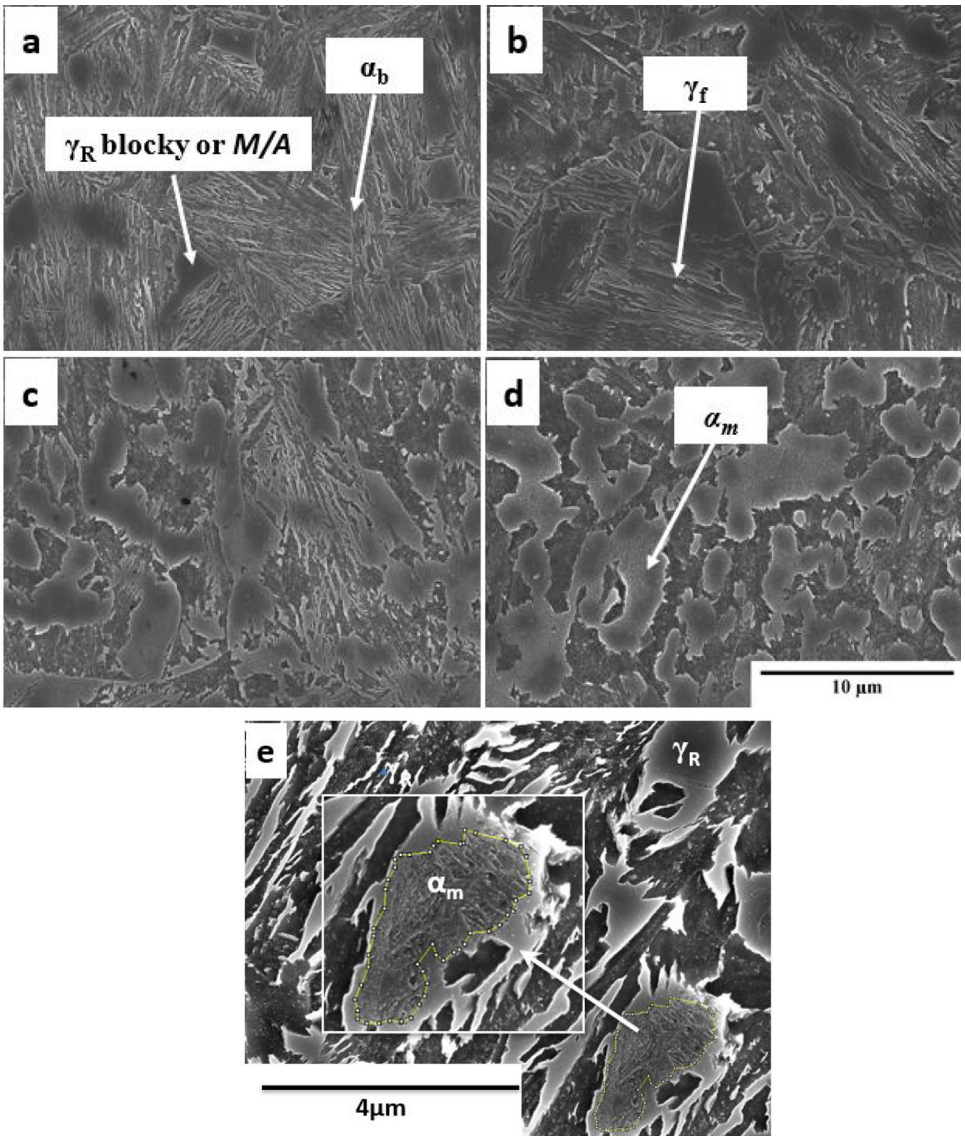

Fig. 5 – SEM micrographs showing a microstructure obtained for the non-ausformed specimens: (a) 325-00, (b) 350-00, (c) 375-00, (d) 400-00, and (e) the contrast between martensite (manually marked by yellow) and retained austenite in M/A constitute. α_b stands for bainitic ferrite, α_m martensite, γ_f and γ_b film and block of retained austenite respectively.

Table 2 – Size of M/A constitutes, and volume fraction of the martensite phase, $V\alpha_{m(SEM)}$, in (%) based on SEM examination and microhardness of non-ausformed and ausformed samples.

TMT condition	Sample code	M/A (μm)	$V\alpha_m$ (SEM)	HV_1
Non-ausforming + austempering	325-00	1.9 ± 0.1	2 ± 0.5	435 ± 9
	350-00	2.1 ± 0.3	4 ± 1.0	408 ± 11
	375-00	3.2 ± 0.5	13 ± 4.0	415 ± 17
	400-00	3.8 ± 0.6	26 ± 3.0	525 ± 18
Ausforming + austempering	325-10	1.7 ± 0.25	2 ± 1	439 ± 6
	325-30	0.8 ± 0.10	2 ± 1	435 ± 6
	325-40	0.8 ± 0.30	3 ± 2	445 ± 5
	350-10	1.9 ± 0.30	10 ± 2	420 ± 13
	350-30	1.4 ± 0.25	12 ± 3	436 ± 12
	375-10	3.4 ± 0.60	17 ± 2	485 ± 17
	375-30	3.6 ± 0.50	21 ± 6	495 ± 17
	400-10	4.3 ± 0.60	33 ± 4	533 ± 16
	400-30	4.5 ± 0.60	35 ± 5	565 ± 20

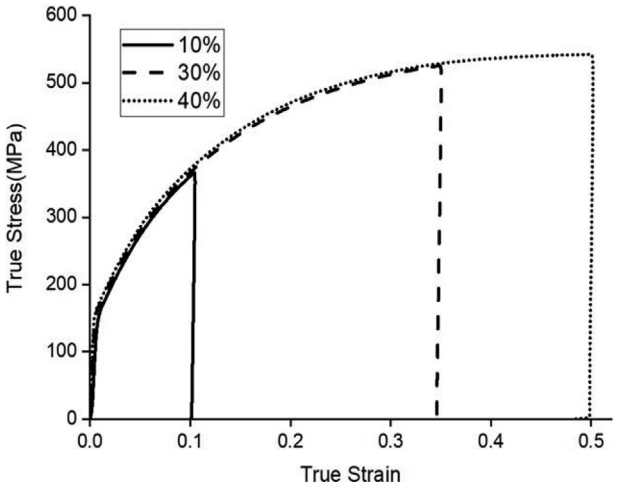

Fig. 6 – Flow curves during ausforming at 600 °C for 10, 30 and 40% deformation.

$$Z = \dot{\varepsilon} \exp\left(\frac{Q}{RT}\right) \quad (6)$$

In the above equations, U refers to the immobilization parameter, and its value is $1.55 \times 10^{15}\ m^{-2}$, and Ω stands for remobilization parameter [51] and equal to 4×10^3 according to Eq. (5), k is a constant with a value taken equal to 180, and m is the exponent for the Zener–Holloman parameter taken equal to −0.1 for austenite in medium carbon steel [52]. The strain rate was equal to $0.1\ s^{-1}$ in the present study, and the activation energy for remobilization, Q, was taken equal to $270\ KJ\ mol^{-1}$ as reported by [52] for medium carbon steel. Finally, R represents the gas constant ($8.31\ J.mol^{-1}\ K^{-1}$), and T the deformation temperature (600 °C).

Using the above equations and constant values, the dislocation densities were calculated for each condition. It can be seen that the dislocation density increased by one order of magnitude when the deformation increased from 10 to 40%. These findings are in agreement with those of Seo et al. [26] who reported that, in medium carbon steel, the dislocation density increased from about $8 \times 10^{+15}$ to about $2 \times 10^{+16}\ m^{-2}$ when the percent deformation of austenite increased 10–50% at 600 °C.

3.3.2. *Dilatometry analysis*

In order to calculate the fraction of martensite formed after the isothermal transformation, $V\alpha_{m(dil)}$, in ausformed samples, a series of experiments were carried out where the samples were quenched immediately after the deformation at 600 °C, rout (D) in Fig. 1b.

Fig. 7a shows the dilatometric curves on cooling to room temperature after deformation was applied as in route (D) in Fig. 1b. The martensitic transformation is occurring in the three tested conditions. While the M_S after 10 and 30% deformation is nearly the same (~310 °C), like that of the no-deformed samples, the results also reveal that the M_S decreases to about 300 °C after 40% of plastic deformation. This slight decrease in the M_S can be rationalized by the significant increase in dislocation density at 40% deformation that would hinder the martensitic transformation through mechanical stabilization and move it to lower temperatures, as also reported by other authors [53–56]. Furthermore, the bainite transformation during cooling from ausforming temperature to isothermal temperature could not be avoided, especially for 30 and 40% deformation, as indicated by arrows in Fig. 7a. This bainitic transformation might be so small that it could be challenging to be observed by microstructural examinations. Note that deforming austenite is known to displace the entire CCT and TTT diagrams toward shorter times, explaining the appearance of bainite on cooling [24,57,58].

An example of the sigmoidal curves during bainitic transformation at 325 and 400 °C after 30% deformation is shown in Fig. 7b. The curves show a similar trend to that of non-ausformed treatments; i.e., the bainitic transformation appears to be completed during the isothermal holding with the RCL reaching a steady-state and the transformation rate reaching almost zero after approximately 1500 s. Moreover, the curves in Figs. 3 and 7c and d, show that ausforming leads to a decrease in the volume fraction of bainite compared with the non-deformed treatments, especially for higher isothermal temperature (400 °C).

It has been reported that as the plastic deformation of austenite increases, so does the dislocation density at the interface between austenite and bainitic ferrite. The increased dislocation density increases the resistance to the growth of the bainitic ferrite plates and could hinder and even stop displacive transformation [59,60]. This resistance becomes more and more significant as the austenite becomes stronger with increased C enrichment resulting in the stabilization of the austenite phase [61]. It must be noted that, as reported by [31,39,58] in addition to mechanical stabilization, preferred ordination due to deformation could also affect the dilatometric signal and produce a similar effect as that of mechanical stabilization. However, the contribution from deformation textures should be minor in the present study as the influence of strain on crystallographic orientation is limited when the supercooled austenite deformed above the bainite start temperature can be considered isotropic [31,62]. Therefore, the dilatation curves can be considered as representative of the bainite transformation.

Fig. 7c and d reveals the dilatometric behavior of the microstructure on cooling to room temperature after isothermal treatment, rout (C) in Fig. 1b. While the sample treated at 325 °C remains unchanged throughout all deformation stages (10 and 30%). However, at 350 °C and higher temperatures, there is a noticeable change in slope linearity even at 10% deformation. The corresponding martensite volume fractions were calculated as already described, and the results thus obtained are presented in Table 2. Together with results in Table 1, it can be said that at 325 °C, the deformation has a minimal effect on the decomposition of retained austenite to martensite as well as on bainitic transformation. However, as the isothermal temperature is increased to 350 °C and above (Fig. 7c), the stability of the retained austenite significantly decreased by introducing even a small amount of deformation. The above changes could be related to the steep decrease in the fraction of the bainitic phase compared to 325 °C. Moreover, the M_S of retained austenite that decomposed to martensite increased with deformation amount probably

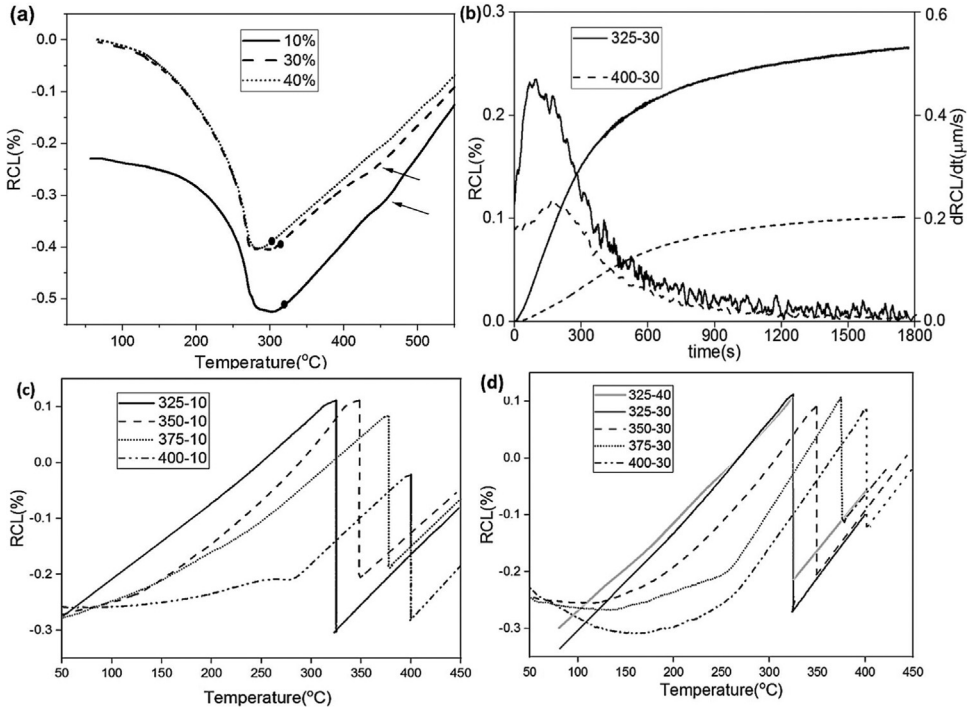

Fig. 7 – (a) Relative change in length vs. temperature during the quenching to room temperature for ausformed samples, (b) the transformation kinetic as function of temperature (325 and 400 °C) and deformation amount (30%), (c) the dilatation behavior during cooling to room temperature after ausforming at 600 °C and isothermal treatment at different temperatures for 10% deformation, (d) for 30 and 40% (black dots indicate the M_s in a).

because the retained austenite has less and less carbon when percent deformation increases. For example, as reported in Table 1, the M_S for sample isothermally treated at 350 °C, increased from a temperature below the room temperature for non-ausformed condition, as seen in Fig. 3 and Table 1, to about 180 °C and 275 °C for 10 and 30% deformation as shown in Fig. 7c and d, respectively. For higher isothermal temperatures (375 and 400 °C), the difference in M_S between 10 and 30% deformation conditions was around 5%.

The above results revealed that retained austenite has higher stability at 325 °C. In order to validate this finding, a new test with a higher deformation level had to be conducted. To this end, various tests were run, and it was found that the maximum achievable deformation at 600 °C in the dilatometer for the investigated alloy was 40%. The results are reported in Fig. 7d (light gray line), where a very slight change in the slope of the dilatation curve can be seen. This minor change can be considered negligible, and therefore, it can be said that the retained austenite is very stable at 325 °C.

3.3.3. *XRD analysis*

The XRD patterns of the 30% deformed samples for the lowest and highest isothermal treatments (325 and 400 °C) are shown in Fig. 8. The XRD spectrum confirms, within the limits of XRD resolution, the absence of any strain induced precipitation and the strong inhibiting role of Si on carbide precipitation [63]. Furthermore, the austenite peak (2 0 0) in Fig. 8 (enlarged image) shows that there was a slight displacement of the diffraction angle (2θ) to the right. This could be an indication of a significant reduction in C_γ concentration for 400-30 samples

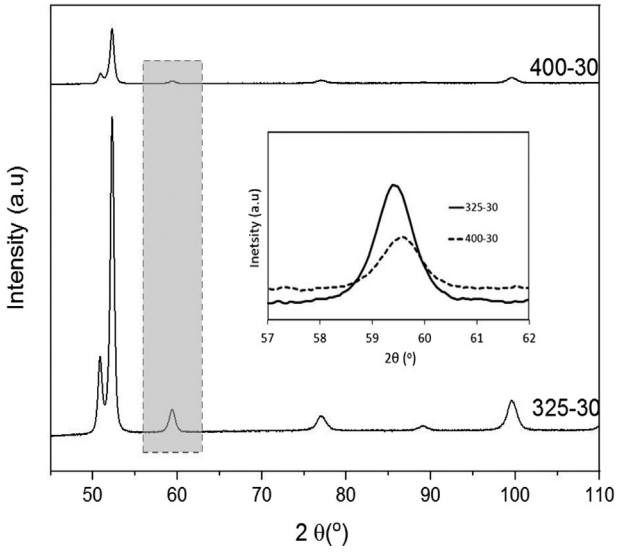

Fig. 8 – XRD diffractogram of ausformed samples 30% deformation, and the inserted image is magnified $\gamma_{(200)}$ spectra for 325-30 and 400-30 samples.

as a result of the substantial delay in the bainitic transformation, due to the higher deformation and isothermal holding temperature. Zhao et al. [41] reported a similar phenomenon in ausformed low-C bainitic steel.

Analysis of the XRD results reported in Table 1, showed that after 10% deformation at 325 °C the bainitic transformation is very slightly affected by the possible mechanical

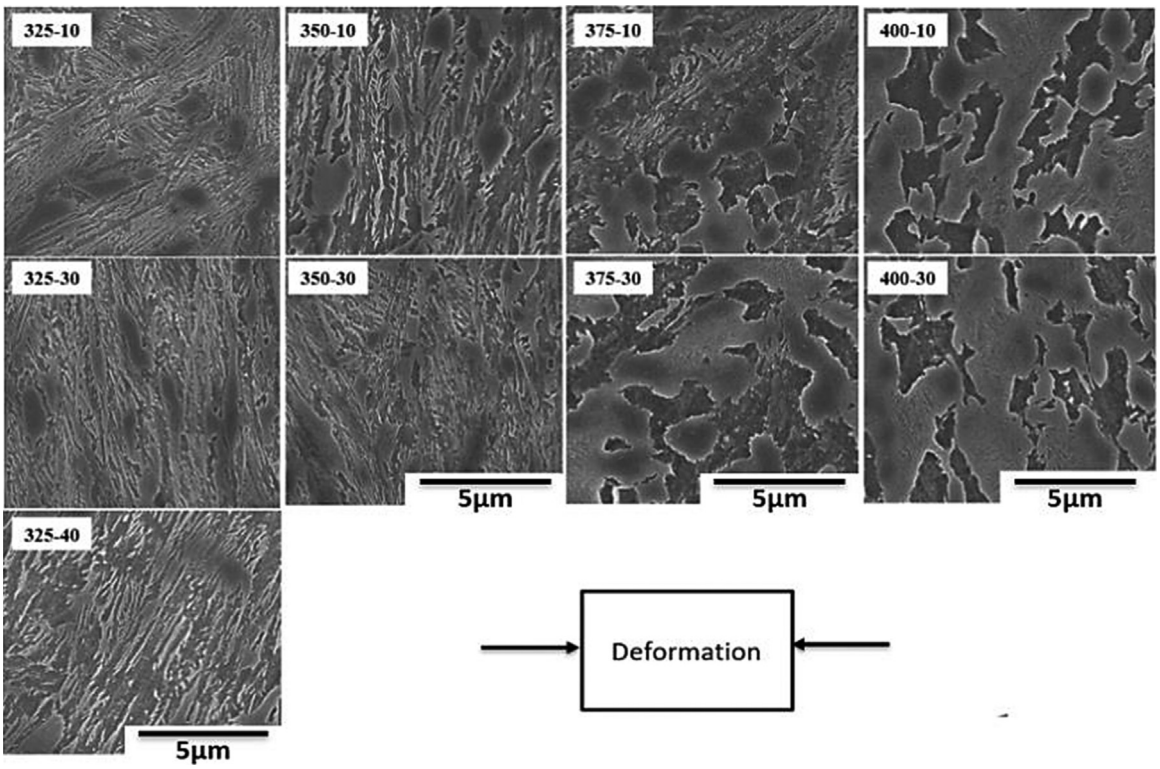

Fig. 9 – SEM images of ausformed samples at 600 °C with different deformation amounts followed by bainitic transformation at different isothermal temperatures.

stabilization of austenite with only a reduction of 4% in the amount of bainite. Nevertheless, after a 40% deformation, the amount of bainite is reduced by more than 10%. At higher isothermal holding temperatures, the stabilization of austenite against bainitic transformation is more visible, although no significant differences are found between the 10 and 30% deformation cases. It must also be noted that, as reported in Table 1, lower degrees of transformation results in higher amounts of martensite.

At higher bainite transformation temperatures, the variation in retained austenite fractions for the ausformed and non-ausformed was minimal, as shown in Table 1. This finding implies that the decomposition of the retained austenite into martensite increased by increasing the amount of deformation, making the volume fraction of retained austenite almost equal for all deformation levels. In contrast, the retained austenite was stabilized for the samples treated at 325 °C, and its volume fraction increased from 14% for the non-ausformed sample to about 23% when the 30% deformation was applied. At 350 °C, there was no evidence that martensite formed during cooling to room temperature for non-ausformed treatment, as shown in the dilatation curve (Fig. 3). However, the decomposition of retained austenite was initiated (Fig. 7c), with the percentage of martensite increasing when the amount of deformation reached 10%, as also presented in Table 1.

3.3.4. *Microstructural and microhardness observations*

SEM micrographs in Fig. 9 reveal the effect of deformation on the retained austenite and martensite evolution after the bainitic transformation has been completed. The presence of blocky-shaped retained austenite along with martensite as well as globular bainite increased with increased deformation and isothermal holding temperatures. The combination of higher isothermal temperature and even a small of deformation, as seen in samples 375-10 and 400-10 (Fig. 9), increased the size of the M/A constituents compared with non-deformed samples, 375-00 and 400-00, as shown in Fig. 5c and d. The latter contains lower carbon, due to the smaller amount of bainitic transformation, compared with lower isothermal temperatures with a large deformation amount (samples 325-30 and 350-30).

The measurements of the size of the M/A constituents were reported in Table 2. It can be seen that the size of M/A constituents increases with the increase in the percent deformation in the case of the 375 and 400 °C isothermal treatments. Whereas, it decreases with increasing the deformation amount for the samples isothermally hold at temperatures lower than 375 °C. The M/A size became finer and reduced by about 50% (~0.8 μm) at 325 °C when the percent deformation increased from 10 to 30%. Thus, based on the above results, as the size of the M/A islands becomes larger, more and more martensite is formed during cooling to room temperature.

The evolution of the microhardness of the ausformed samples is also reported in Table 2. It can be seen that independently of the testing temperature, the hardness increases with percent deformation though the increase in hardness became more evident when the bainitic transformation temperature increased. For instance, at 325 °C, the hardness was almost constant for the samples 325-10 and 325-30 (less than 1% dif-

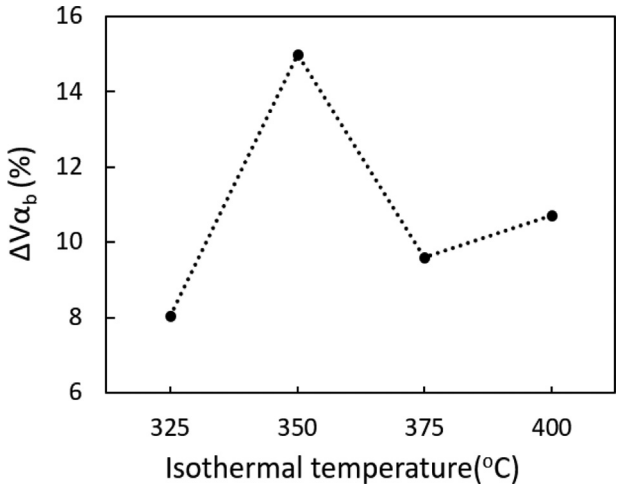

Fig. 10 – Difference in bainite volume fractions between non-ausformed and 10% ausformed samples for different bainite transformation temperatures.

ference) owing to the limited effect of deformation on the bainite volume fraction for both samples. However, for treatment at 350 °C, the hardness continuously increased from 420 to about 436 HV for samples 350-10 and 350-30, respectively. The increase in hardness is probably related to the increase of transformed martensite from 10 to 12% for samples 350-10 and 350-30, respectively, as well as the higher dislocation density for 30% deformation, as discussed earlier. The combination of higher isothermal temperature and the percentage deformation led to a cessation in the bainitic transformation and resulted in a higher amount of martensite, thus leading to a significant increase in hardness (above 500 HV), as measured in samples 375-30 and 400-30. Furthermore, it must be noted that the error ranges of hardness measurements were more significant for the highly deformed samples (30 and 40%) and higher isothermal temperatures (375 and 400 °C), probably due to the presence of martensite islands that are non-uniformly distributed in the samples, resulting in a less homogeneous microstructure.

Based on the obtained results, the test condition corresponding to 10% ausforming followed by isothermal treatment at 350 °C appears to be a threshold, below and above which the effect of deformation on the stability of retained austenite is different. To further validate this finding, the difference in bainite volume fraction transformed at different isothermal temperatures for ausformed (10% deformation) and non-ausformed samples was calculated, and it was found that the most substantial difference was observed in sample 350-10, as shown in Fig. 10. This could explain why the effect of deformation on retained austenite stability was also more noticeable in 350-10 samples.

In summary, the mechanism of the effect of deformation on the stability of retained austenite could be classified into three stages, as schematically illustrated in Fig. 11. At the isothermal temperature of 325 °C, the deformation effect is minimal and could be neglected. This can be explained by the presence of higher bainitic volume fractions. This is due to the high driving force at low transformation temperatures, which overcome the resistance of the bainitic sheave growth because of the introduction of either small (10%) or large (40%) deformation.

At 375 and 400 °C temperatures, as seen in Fig. 11b, the reductions in retained austenite stability were directly proportional to the amount of deformation. However, it is difficult to accurately quantify the effect of strain on retained austenite stability compared with non-deformed ones, due to the

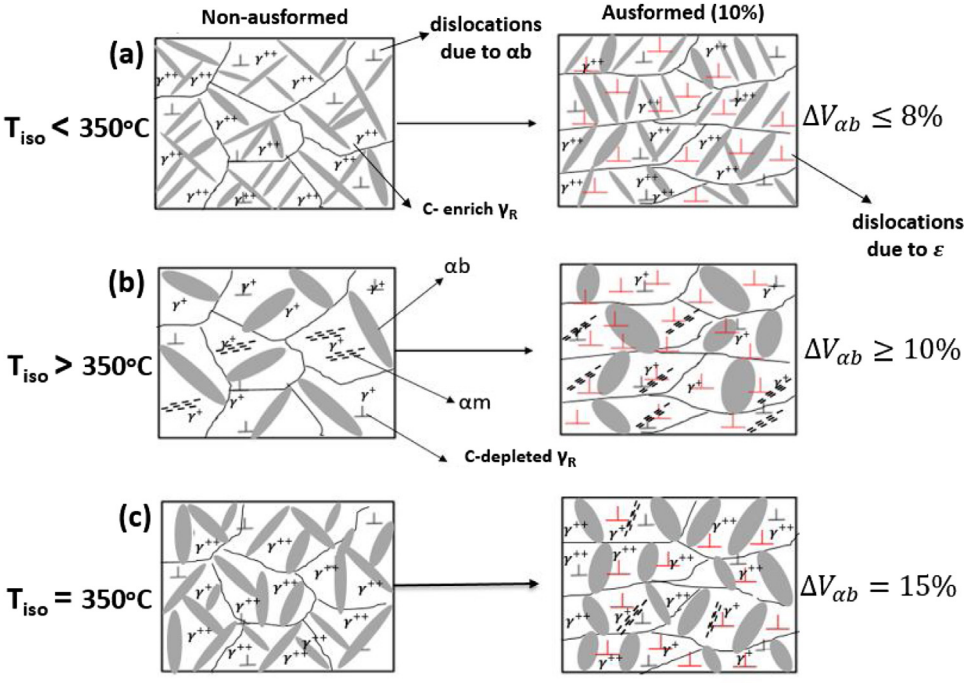

Fig. 11 – Schematic graph of the effect of deformation on the stability of retained austenite, (a) below 350 °C, (b) above 350 °C, (c) at 350 °C.

presence of the martensite phase, even for non-ausformed samples submitted to pure isothermal transformation.

At 350 °C, as shown in Fig. 11c, the results showed that the retained austenite was stable for non-ausformed isothermal treatment, and the amount of transformed martensite was negligible. However, this stability was reduced, and the amount of martensite increased substantially, after 10% deformation. Specifically, in this case, the bainite volume fraction and C_{γ_R} increased to above 14 and 15%, respectively. Under these conditions, dislocation resistance to the growth of bainitic sheaves overcome the bainite nucleation rate, as also reported in [57]. As a result, the large islands of retained austenite contained less carbon, which transformed to martensite at a higher M_S and distributed among the bainite sheaves.

4. Conclusions

In the present study, the effect of ausforming on the stability of retained austenite and its decomposition to martensite after the completion of isothermal holding treatment in medium C–Si steel was investigated. The following conclusions can be drawn from this study:

1) The amount of transformed bainite is a critical parameter controlling the decomposition of retained austenite to martensite during cooling to room temperature.
2) In pure isothermal treatments (non-ausformed), the isothermal holding temperature of 350 °C can be considered as the threshold temperature for retained austenite stability. At 350 °C and below, the retained austenite is very stable, and above it, the retained austenite is unstable.
3) For ausformed samples, the decomposition of retained austenite to martensite can be altered via a small deformation amount (10%) at and above the threshold temperature (i.e., 350 °C). Whereas, at a lower temperature, the retained austenite is very stable, regardless of percent deformation.
4) Above 350 °C, ausforming enhances the formation of blocky-shaped retained austenite that contains lower carbon content than the film-like retained austenite morphology, resulting in increased martensitic transformation during cooling to room temperature.
5) At lower isothermal transformation temperatures (325 and 350 °C), the blocks were thinner with increased percent deformation.

Conflicts of interest

The authors declare that they have no known competing financial interests or personal relationships that could have appeared to influence the work reported in this paper.

Acknowledgments

This research was supported by the Ministry of Higher Education and Scientific Research in Libya with the collaboration with the Canadian Bureau for International Education (CBIE). The author also would like to thank Adriana Eres-Castellanos from CENIM-CSIC in Spain, for her informative scientific support.

REFERENCES

[1] Bhadeshia HKDH. Nanostructured bainite. Proc Roy Soc A: Math Phys Eng Sci 2009;466(2113):3–18.
[2] Caballero FG, Bhadeshia HKDH. Very strong bainite. Curr Opin Solid State Mater Sci 2004;8(3–4 (Jun–Aug)):251–7.
[3] Garcı-Mateo C, Caballero FG. The role of retained austenite on tensile properties of steels with bainitic microstructures. Mater Trans 2005;46(8 (Aug)):1839–46.
[4] Spanos G, Fang HS, Aaronson HI. A mechanism for the formation of lower bainite. Metall Trans A 1990;21(6 (Jun)):1381–90.
[5] Cornide J, Garcia-Mateo C, Capdevila C, Caballero FG. An assessment of the contributing factors to the nanoscale structural refinement of advanced bainitic steels. J Alloys Compd 2013;577(Nov):S43–7.
[6] Singh SB, Bhadeshia HKDH. Estimation of bainite plate-thickness in low-alloy steels (in English). Mater Sci Eng A 1998;245(1 (Apr)):72–9.
[7] Bhadeshia HKDH, Edmonds DV. Bainite in silicon steels: new composition-property approach. Part1. Min Met Mater Soc 1983.
[8] Xie ZJ, Ren YQ, Zhou WH, Yang JR, Shang CJ, Misra RDK. Stability of retained austenite in multi-phase microstructure during austempering and its effect on the ductility of low carbon steel. Mater Sci Eng A 2014;603(May):69–75.
[9] Grajcar A, Skrzypczyk P, Kozłowska A. Effects of temperature and time of isothermal holding on retained austenite stability in medium-Mn steels. Appl Sci 2018; 8(11 (Nov)).
[10] Podder AS. "Tempering of a Mixture of Bainite and Retained Austenite," thesis. University of Cambridge, Department of Materials Science and Metallurgy; 2011.
[11] Xiong BCXC, Huang MX, Wanga JF, Wang L. The effect of morphology on the stability of retained austenite in a quenched and partitioned steel. Scr Mater 2013.
[12] Luo H, Shi J, Wang C, Cao W, Sun X, Dong H. Experimental and numerical analysis on the formation of stable austenite during the intercritical annealing of 5Mn steel. Acta Mater 2011;59(10 (Jun)):4002–14.
[13] Lee S, Lee S-J, De Cooman BC. Austenite stability of ultrafine-grained transformation-induced plasticity steel with Mn partitioning. Scr Mater 2011;65(3 (Aug)):225–8.
[14] Chiou CS, Yang JR, Huang CY. The effect of prior compressive deformation of austenite on toughness property in an ultra-low carbon bainitic steel. Mater Chem Phys 2001;69(1–3 (Mar)):113–24.
[15] Leijie Zhao LQ, Zhou Q, Li D, Wang T, Jia Z, Zhang F, et al. The combining effects of ausforming and below-M_s or above-M_s austempering on the transformation kinetics, microstructure and mechanical properties of low-carbon bainitic steel. Mater Des 2019;183(5 (December)):108123.
[16] Miihkinen VTT, Edmonds DV. Tensile deformation of two experimental high-strength bainitic low-alloy steels containing silicon. Mater Sci Technol 2013;18(6 (Jul)): 432–40.
[17] Tian J, Xu G, Jiang Z, Wan X, Hu H, Yuan Q. Transformation behavior and properties of carbide-free bainite steels with different Si contents. Steel Res Int 2018;90(3 (December)).
[18] Klein T, Lukas M, Haslberger P, Friessnegger B, Galler M, Ressel G. Complementary thermal analysis protocols for the investigation of the tempering reactions of a carbide-free bainitic steel. JOM 2019;71(4 (Apr)):1357–65.

[19] Wu HD, Miyamoto G, Yang ZG, Zhang C, Chen H, Furuhara T. Incomplete bainite transformation in Fe–Si–C alloys. Acta Mater 2017;133(Jul):1–9.
[20] Varshney A, Sangal S, Kundu S, Mondal K. Super strong and highly ductile low alloy multiphase steels consisting of bainite, ferrite and retained austenite. Mater Des 2016;95(5 (Apr)):75–88.
[21] Mingxing Zhou G, Zhang Y, Xue Z. The effects of external compressive stress on the kinetics of low-temperature bainitic transformation and microstructure in super bainite steel. Int J Mater Res 2015.
[22] Zhou XTSYX, Lianga JW, Shena YF, Misrab RDK. Innovative processing of obtaining nanostructured bainite with high strength – high ductility combination in low-carbon–medium-Mn steel: process–structure–property relationship. Mater Sci Eng A 2018.
[23] Zhao L, et al. Producing superfine low-carbon bainitic structure through a new combined thermo-mechanical process (in English). J Alloys Compd 2016;15(685 (Nov)):300–3.
[24] Zhao J, et al. Transformation behavior and microstructure feature of large strain ausformed low-temperature bainite in a medium C – Si-rich alloy steel. Mater Sci Eng A 2017;682(Jan):527–34.
[25] Hu H, Xu G, Wang L, Zhou M. Effects of strain and deformation temperature on bainitic transformation in a Fe–C–Mn–Si alloy. Steel Res Int 2017;88(3 (Mar)).
[26] Seo SW, Jung GS, Lee JS, Bae CM, Bhadeshia HKDH, Suh DW. Ausforming of medium carbon steel. Mater Sci Technol 2015;31.
[27] Maalekian M, Kozeschnik E, Chatterjee S, Bhadeshia HKDH. Mechanical stabilization of eutectoid steel. Mater Sci Technol 2013;23(5):610–2.
[28] Bhadeshia HKDH. Bainite in steels, theory, and practice. 3rd ed. University of Cambridge and POSTECH; 2015.
[29] U. Sente Software Ltd, JMarPro the Materials Property Simulation Package, Version 9.0.
[30] T. instruments, DIL 805A/D, 2018.
[31] Eres-Castellanos A, Morales-Rivas L, Latz A, Caballero FG, Garcia-Mateo C. Effect of ausforming on the anisotropy of low-temperature bainitic transformation. Mater Charact 2018;145:371–80, 11/01/2018.
[32] Jatczak CF. Retained austenite and its measurement by X-ray diffraction. SAE International; 1980. February 25–29.
[33] Navarro-Lo' pez JSA, Santofimia MJ. Effect of prior athermal martensite on the isothermal transformation kinetics below M_s in a low-C high-Si steel. Metall Mater Trans A 2015;29(December).
[34] Saha Podder A, Bhadeshia HKDH. Thermal stability of austenite retained in bainitic steels. Mater Sci Eng A 2010;527(7–8 (Mar)):2121–8.
[35] Navarro-López A, Hidalgo J, Sietsma J, Santofimia MJ. Influence of the prior athermal martensite on the mechanical response of advanced bainitic steel. Mater Sci Eng A 2018;735(Sep):343–53.
[36] Asia NP. MIP (Metallographical Image Processing); 2018. http://metsofts.com/.
[37] Yang H-S, Bhadeshia HKDH. Uncertainties in dilatometric determination of martensite start temperature. Mater Sci Technol 2013;23(5 (May)):556–60.
[38] Santajuana, et al. Quantitative assessment of the time to end bainitic transformation. Metals 2019;9(9 (Sep)).
[39] Liu M, Ma Y, Xu G, Cai G, Zhou M, Zhang X. Effects of plastic stress on transformation plasticity and microstructure of a carbide-free bainite steel. Metallogr Microstruct Anal 2019;8(2 (January)):159–66.
[40] Koo M, Xu P, Tomota Y, Suzuki H. Bainitic transformation behavior studied by simultaneous neutron diffraction and dilatometric measurement (in English). Scr Mater 2009;61(8 (Oct)):797–800.
[41] Zhao L, et al. The combining effects of ausforming and below-M_s or above-M_s austempering on the transformation kinetics, microstructure and mechanical properties of low-carbon bainitic steel. Mater Des 2019;183(Dec).
[42] Zhi C, Zhao A, He J, Yang H, Qi L. Effects of the multi-step ausforming process on the microstructure evolution of nanobainite steel. In: International Conference on Advanced Materials, Structures and Mechanical Engineering. 2015. p. 399–403.
[43] Suh D-W, Oh C-S, Han HN, Kim S-J. Dilatometric analysis of austenite decomposition considering the effect of non-isotropic volume change. Acta Mater 2007;55(8 (May)):2659–69.
[44] Liu B, Li W, Lu X, Jia X, Jin X. The effect of retained austenite stability on impact-abrasion wear resistance in carbide-free bainitic steels. Wear 2019;428–429:127–36.
[45] Bhadeshia HKDH. New bainitic steels by design. Miner Met Mater Soc 1989:69–78.
[46] Bhadeshia HKDH. High-performance bainitic steels. Mater Sci Forum 2005;500–501(November):63–74.
[47] Navarro-López A. Influence of the prior athermal martensite on the mechanical response of advanced bainitic steel; 2018. p. 343–53.
[48] Garcia-Mateo C, Caballero FG, Bhadeshia HKDH. Acceleration of low-temperature bainite. ISIJ Int 2003;43(11):1821–5.
[49] Li Z-D, Yang Z-G, Zhang C, Liu Z-Q. Influence of austenite deformation on ferrite growth in a Fe–C–Mn alloy. Mater Sci Eng A 2010;(May):4406–11.
[50] Bergström Y. A dislocation model for the stress–strain behavior of polycrystalline α-Fe with special emphasis on the variation of the densities of mobile and immobile dislocations. Mater Sci Eng 1970;5(4 (March)):193–200.
[51] Bodin A, Sietsma J, van der Zwaag S. Flow stress prediction during intercritical deformation of low-carbon steel with a rule of mixtures and Fe-simulations. Scr Mater 2001;45(8 (Oct)):875–82.
[52] Li Z-D, Yang Z-G, Zhang C, Liu Z-Q. Influence of austenite deformation on ferrite growth in a Fe–C–Mn alloy. Mater Sci Eng A 2010;527(16–17 (June)):4406–11.
[53] Garcia-Mateo C, Caballero FG, Chao J, Capdevila C, Garcia de Andres C. Mechanical stability of retained austenite during plastic deformation of super high strength carbide free bainitic steels. J Mater Sci 2009;44(17 (Sep)):4617–24.
[54] Nikravesh M, Naderi M, Akbari GH. Influence of hot plastic deformation and cooling rate on martensite and bainite start temperatures in 22MnB5 steel. Mater Sci Eng A 2012;540(April):24–9.
[55] Zhang M, Wang YH, Zheng CL, Zhang FC, Wang TS. Austenite deformation behavior and the effect of ausforming process on martensite starting temperature and ausformed martensite microstructure in medium-carbon Si–Al-rich alloy steel. Mater Sci Eng A 2014;596(Feb):9–14.
[56] Zhang M, Wang YH, Zheng CL, Zhang FC, Wang TS. Effects of ausforming on isothermal bainite transformation behavior and microstructural refinement in medium-carbon Si–Al-rich alloy steel. Mater Des 2014;62(September):168–74.
[57] Hu H, Zurob HS, Xu G, Embury D, Purdy GR. New insights to the effects of ausforming on the bainitic transformation. Mater Sci Eng A 2015;626(Feb):34–40.
[58] Gong W, Tomota Y, Adachi Y, Paradowska AM, Kelleher JF, Zhang SY. Effects of ausforming temperature on bainite transformation, microstructure and variant selection in nanobainite steel. Acta Mater 2013;61(11 (Jun)):4142–54.
[59] Shipway PH, Bhadeshia HKDH. Mechanical stabilization of bainite, (in English). Mater Sci Technol 2013;11(11 (Nov)):1116–28.

[60] Chatterjee S, Wang H-S, Yang JR, Bhadeshia HKDH. Mechanical stabilization of austenite. Mater Sci Technol 2013;19(Jul):641–4.
[61] Yoozbashi MN, Yazdani S, Wang TS. Design of a new nanostructured, high-Si bainitic steel with lower-cost production. Mater Des 2011;32(6 (Jun)):3248–53.
[62] Fan H-L, Zhao A-M, Li Q-C, Guo H, He J-G. Effects of ausforming strain on bainite transformation in nanostructured bainite steel. Int J Miner Metall Mater 2017;24(3 (Mar)):264–70.
[63] Tian J, Xu G, Jiang Z, Wan X, Hu H, Yuan Q. Transformation behavior and properties of carbide-free bainite steels with different Si contents. Steel Res Int 2018;90(3 (December)):1800–2474.